in *Infrared Astronomical Instrumentation*, ed A.M. Fowler, *Proceedings SPIE*, *3354*, 57 (1998).

Far-infrared imaging array for SIRTF

E.T. Young, J.T. Davis, C.L. Thompson, G.H. Rieke, G.Rivlis,
R. Schnurr, J. Cadien, L. Davidson, G. S. Winters, and K. A. Kormos
Steward Observatory, University of Arizona, Tucson AZ 85721

ABSTRACT

We describe the design, construction, and performance of the 32x32 Ge:Ga imaging array being built at the University of Arizona for the Multiband Imaging Photometer for SIRTF (MIPS). The array will support a number of operational modes in the MIPS instrument including natural background-limited mapping at 70 μm, super-resolution observations at 70 μm, and spectral energy distribution measurements between 50 and 100 μm. The array is constructed in a modular manner using eight 4x32 pixel building blocks. To meet the sensitivity and stability requirements, the array must have excellent photometric repeatability, low noise, and robustness to the effects of the ionizing radiation environment in space. Key elements in attaining this level of performance are the Ge:Ga detectors materials and the cryogenic CRC-696 readout electronics. We present laboratory data for a 16x32 prototype of the array, and describe the plans for the construction of the qualification and flight units.

1. INTRODUCTION

The Space Infrared Telescope Facility (SIRTF) will be the premier infrared astronomical facility in the first half of the coming decade. The 85-cm cryogenically cooled telescope is scheduled to be launched into a solar orbit in late 2001, where it will conduct imaging and spectroscopic observations. Free of the heat load from the Earth, SIRTF will operate for an anticipated 5 year mission. Also, the great reduction in Earth avoidance constraints compared to previous low-earth orbit observatories means greatly simplified operations and a significantly higher observing efficiency. While the solar orbit is the critical factor in attaining the long lifetime and high efficiency, the key to the scientific productivity will be the sensitive, large format detector arrays on SIRTF.

The goal of our development has been to extend large format, high sensitivity array technology into far infrared. We describe the design, construction, and performance of the 32 x 32 Ge:Ga array for the Multiband Imaging Photometer for SIRTF (MIPS). This array operates in the wavelength range 50 - 100 μm. In a companion paper, Schnurr et al.[1] Describe the design of the stressed Ge:Ga array that operates at 160 μm. Previously[2, 3], we have described the construction of the basic building block for this array, the 4 x 32 pixel Z-plane module. We have produced a number of modules and have successfully built a 16 x 32 stacked array.

As has been well demonstrated by the Infrared Astronomical Satellite (IRAS) and the Infrared Space Observatory (ISO), the far infrared is essential in understanding a wide variety of astronomical phenomena. Ultraluminous infrared galaxies emit the bulk of their power at far infrared wavelengths. The youngest protostars are primarily far infrared sources. Excess emission in the far infrared will be the characteristic signature of cool debris disks around stars. SIRTF is the only planned facility that will combine a very cold telescope (<< 10 K) with at sizable detector arrays; although they are much larger, the future capabilities such as the Stratospheric Observatory for Infrared Astronomy (SOFIA), the Far Infrared Space Telescope (FIRST), and the Next Generation Space Telescope (NGST) will all have much warmer telescopes that will suffer at the longest wavelengths. Hence, a special motivation in our array design has been to produce a detector that takes full advantage of the SIRTF conditions by being only limited by the natural backgrounds.

2. PERFORMANCE REQUREMENTS

As a necessary simplification, MIPS will have no filter wheel mechanism. Hence, the operating wavelength for the far infrared array is a very important consideration. The choice of 70 μm was driven by the desire to go to the longest wavelength that is not confusion noise limited in reasonably long integration times. The pixel scale of 9.4 arc seconds provides good sampling of the point spread function ($\lambda / 1.8$ D), while the 32 x 32 format provides a useful 5' x 5' field of view for mapping. Given the COBE measurements of the infrared background[4], we have computed the detector performance required to satisfy the

background limited criterion. For a nominal 50% instrumental optical transmission, the required Noise Equivalent Flux Density is 130 μJy in a 2000 s integration viewing the darkest sky locations. At the detector this requirement translates to a Noise Equivalent Power of 2.5 x 10^{-18} W $Hz^{-½}$ at a background power of 2.2 x 10^{-17} W. This NEP can be achieved with a variety of plausible detector parameters. For example, an increase in detector responsivity would allow an increase in both read noise and dark current without sensitivity penalty. We have recast our ***derived*** detector performance requirements such as dark current and read noise into a form that allows a tradeoff between various parameters. To satisfy the basic sensitivity goals, we have:

$$\mathbf{D.Q.E.} > 0.05 / e \qquad 1)$$

$$i_{dark} < 38 * \boldsymbol{S} \quad (e/s) \qquad 2)$$

$$\text{Read Noise} < 38 * \boldsymbol{S} \quad (e) \qquad 3)$$

Where **D.Q.E.** is the detective quantum efficiency, e is the instrument efficiency, i_{dark} is the dark current in units of e/s, ***S*** is the Responsivity in units of Amp/Watt, and read noise is in units of electrons.

The scientific utility of the measurements also depends on the repeatability of the observations. To meet the science requirements, we require repeatability to better than 4% for bright objects. Since SIRTF will be in an ionizing radiation environment, some method of mitigating the change in photoconductor responsivity is required. Our laboratory tests have demonstrated that thermal annealing to >7K is the most effective method for restoring the responsivity to pre-irradiation levels. Our array design includes provisions for annealing the detectors with a minimal impact on both observing efficiency and helium lifetime.

The other consequence of space observations is the effect of galactic cosmic rays on the sensitivity of the detectors. The predicted fluence of cosmic rays is ~4 protons s^{-1} cm^{-2} . Each cosmic ray deposits a significant charge in the detector that causes a momentarily large photocurrent in the detector and can possibly upset baselines. Moreover, the disturbing hit can potentially crosstalk to neighboring detectors. For the MIPS array the choice of Capacitive Transimpedance Amplifier (CTIA) readouts greatly reduces these disturbing effects.

Finally, the array must, of course, satisfy all the environmental, interface, and quality assurance requirements of the mission. The array performance requirements are summarized in Table 1, along with a set of derived parameters for ε= 50% and S=5 A/W.

3. DESIGN DESCRIPTION

The design of the 4x32 modules has been described in detail by Young , Scutero et al.[2]. The main components of the module are a 4x32 detector assembly, a ceramic multilayer board (CMLB) which holds the readouts and ancillary passive components, a molybdenum frame, and a flex cable for electrical interconnect. To make a complete array, eight of the modules are stacked on an array mount. The mount includes a multilayer flex cable with connectors that provides the electrical interface between the focal plane modules and the cryostat wiring.

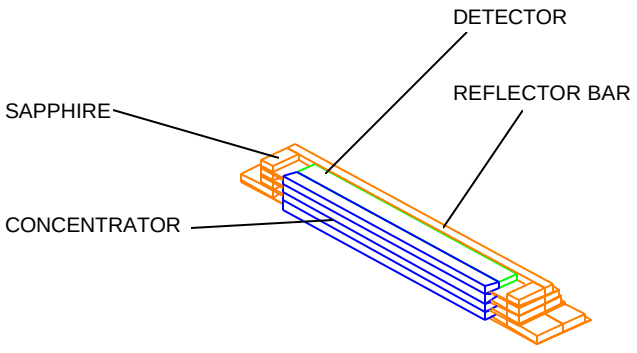

Figure 1 Detector Assembly Components

3.1 Detectors

The MIPS focal plane array uses high performance Ge :Ga detector material grown at Lawrence Berkeley Laboratory. The Ge:Ga, which comes from Boule 113, has a typical Ga concentration of ~ 2 x 10^{14} cm^{-3}. The detectors are arranged in strips of 1 x

32 elements mounted on 125 μm thick sapphire substrates (See Figure 1). The detector strips are 25.5 mm long, 2 mm deep, and 0.5 mm thick. The 25.5 mm length is divided electrically into 34 pixels (32 active and 2 guard) by photolithography. Photon absorption takes place along the 2 mm direction, hence the active pixel area is 0.75 mm x 0.5 mm. To expand the pixel size to the desired 0.75 mm x 0.75 mm, we utilize germanium optical concentrators that act as solid feed horns into the detectors. It is interesting to note that the joint between the concentrator and the detector acts as a multilayer stack, with peaks and nulls in the transmission as a function of wavelength. By maintaining close tolerance (gap less than 3 μm) on the contact region between the detector and the concentrators, however, the collection efficiency is acceptably high.

3.2 Readouts

The CRC-696 readout is the result of a long development activity to produce devices that operate with good DC stability and low noise in the sub freezeout regime. The initial devices were produced at the former Hughes Technology Center, Carlsbad CA. Subsequent runs have been produced at the Raytheon Newport Beach foundry. The mask set for the CRC-696 contains a number of circuit variations including the familiar Source Follower per Detector (SFD) and the Capacitive Transimpedance Amplifier (CTIA). For the MIPS array, the CTIA is the clear choice for a number of reasons. First, with the CTIA the transconductance is much higher than with the SFD. With a feedback capacitor of only 36 fF, the CTIA has a transconductance of 4 μV/ electron compared with ~0.1 μV/ electron for the SFD. Consequently, the noise requirements for the following stages is much less severe for the CTIA. Second, the bias on the detector is constant during an integration. The possible voltage change on the input node during an integration is reduced by the very large loop gain of the CTIA. Since the operating voltage of the germanium detectors is quite low, this debiasing would severely limits the full well capacity of the array. Also, this bias constancy proves to be very important in maintaining detector performance in a radiation environment. Finally, since the input node is at a constant potential because of the feedback, there is essentially no electrical crosstalk in this focal plane array. The CRC-696 CTIA readout has attained a bare mux read noise of 28 e^- at a temperature of 2 K.

Table 1 Focal Plane Performance Requirements

	Required	**Achieved**
Detective Quantum Efficiency	>10%	>20%
Responsivity	>5 A/W	~7 A/W
Dark Current	< 190 e/s	<200 e/s
Read Noise (mean)	<100 e	~100 e
Well Depth	>160,000 e	~270,000 e
Crosstalk	<15%	<1%
Fill Factor	>90%	>95%
Uniformity	+/-30%	~30%
Power Dissipation	<2.5 mW	1.3 mW
Radiation Dose	2.5 Krad	>15 Krad
Power to Anneal to 8K, 10s every hour	<1 mW average	0.9 mW average

3.3 Ceramic Multilayer Board

The ceramic multilayer board (CMLB) holds the four CRC-696 readouts, bypass capacitors, and ground sense resistors. It also provides the interconnect between the readouts and the output flex cable. To minimize electrical noise pickup, the digital clock lines are contained within ground planes. Figure Figure 2 shows the layout of the CMLB. The detectors are directly wire bonded to the readout inputs at the bottom of the figure, and the output cable is wire bonded to the pads at the top of the figure.

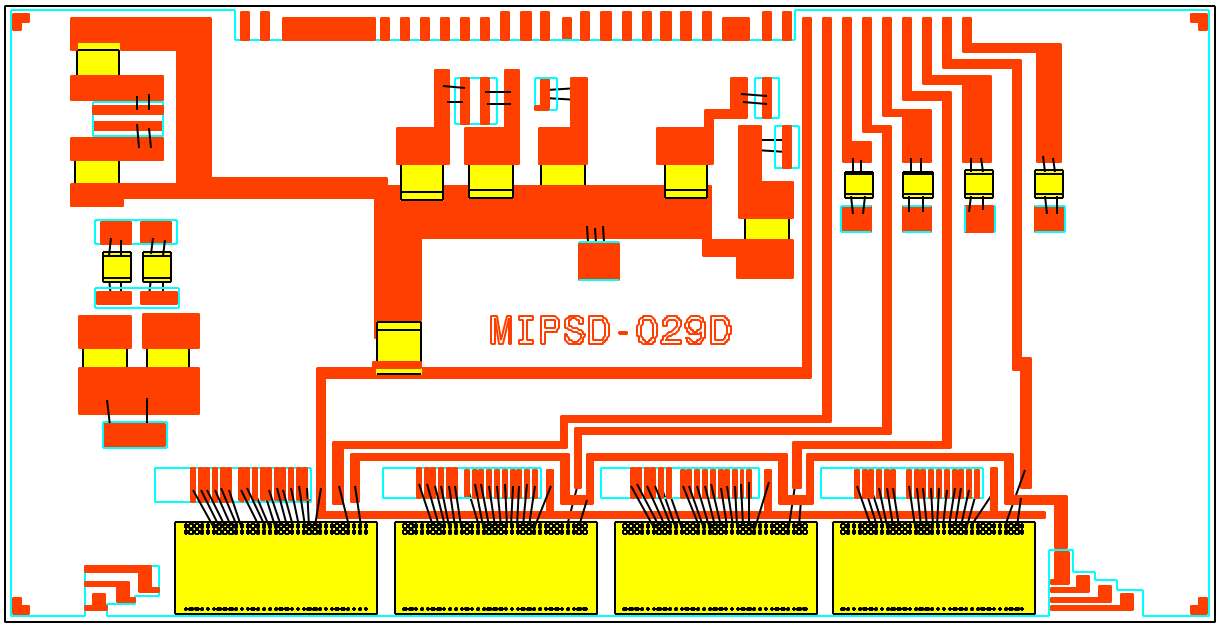

Figure 2 Ceramic Multilayer Board Layout

3.4 Flex Cable

The flex cable is a simple 37-conductor cable with ground plane. The cable has a Nano connector at the output and incorporates a ground plane for shielding.

3.5 Molybdenum Frame

The molybdenum frame acts a the carrier for the front end detector assembly, ceramic multilayer board, and the output flex cable. This material was chosen for its combination of excellent thermal conductivity at low temperatures and its coefficient of thermal expansion match with sapphire and germanium. The thickness of the molybdenum frame is exactly the same as four rows of pixels, allowing the modules to be closely stacked into a filled 2-dimensional array. Figure 3 shows the major components of the full 4x32 module.

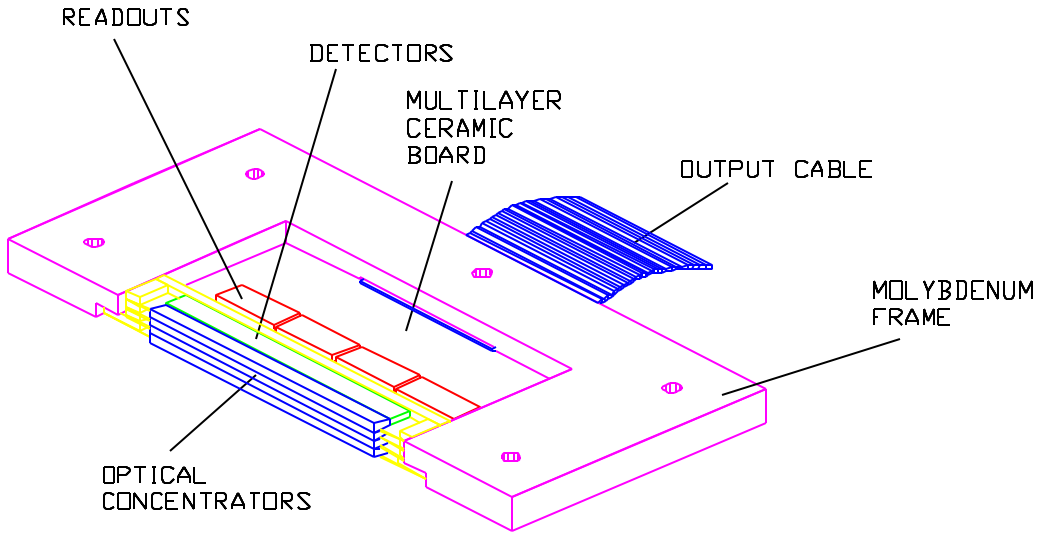

Figure 3 4x32 Module Major Components

3.6 Backplane Assembly

The backplane assembly is the carrier that holds the 4x32 modules. It consists on a molybdenum bottom plate, flex cable backplane, and a housing. The flex cable backplane has eight nano connectors that match the connectors on the 4x32 modules. The backplane assembly with nano connectors is shown in Figure 4. The redundancy philosophy for MIPS requires that the loss of any single wire cannot disable completely an instrument function. Consequently, the Ge:Ga focal plane is divided into two electrically independent halves. The "A" half consists of modules 1-4, while the "B" half consists of modules 5-8. Within each half, the bias and address lines are commoned. Each CRC-696 readout has an independent output and ground return. Hence the full array has 32 parallel outputs. The 32x32 array has four output connectors. A pair of 37-pin micro-D connectors carry the detector output signals along with their associated ground lines; a pair of 51-pin micro-D connectors carry the address, bias, and housekeeping lines.

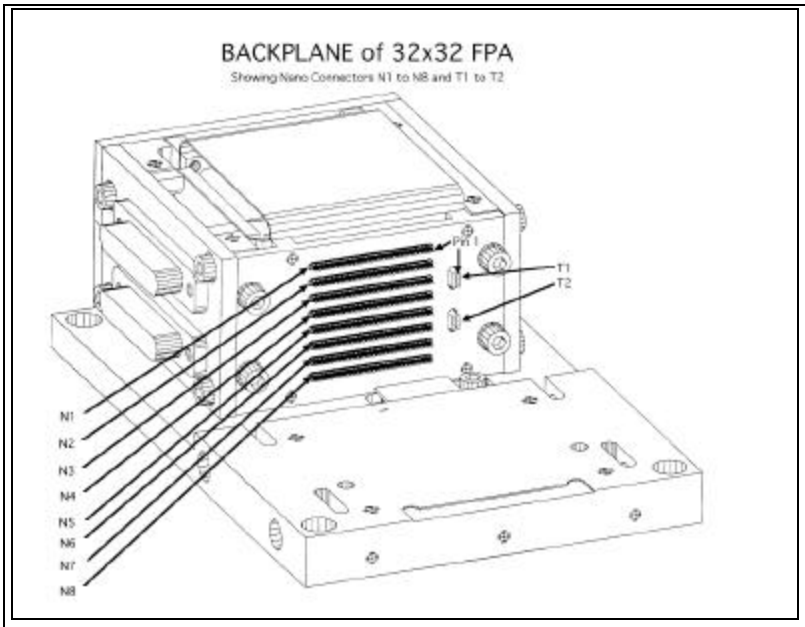

Figure 4 32x32 Backplane Assembly

Figure 5 depicts the assembled 32x32 Ge:Ga focal plane array.

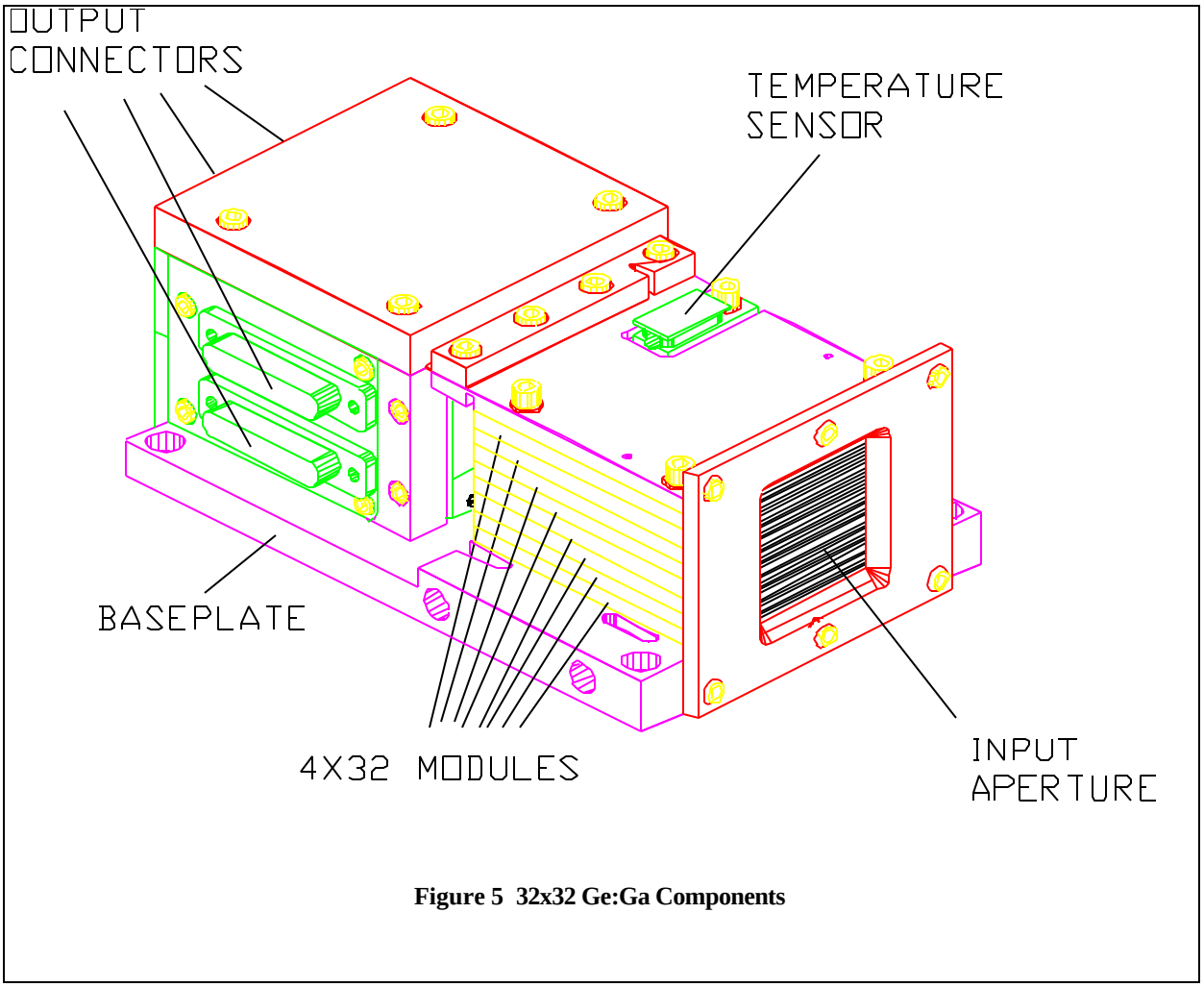

Figure 5 32x32 Ge:Ga Components

4. TEST RESULTS

The bulk of the testing for this program has been done at the 4x32 module level. Since each module is electrically independent, with four independent outputs, module testing should be representative of the expected performance of the fully assembled array. Additionally, we report the results of a 16x32 stack of four modules. The principal parameters tested in our standard screening are dark current, read noise, and responsivity. Additional important items characterized are well depth, power dissipation, output impedance, and anneal performance.

4.1 Read Noise

The read noise is determined under dark conditions. The array is non-destructively sampled eight times per second for an integration time of eight seconds. For the sample-up-the-ramp measurement, the photocurrent is proportional to the slope of the output voltage vs. time. The read noise is then defined as the product of the standard deviation of the ensemble of slopes and the integration time. Figure 6 shows the read noise distribution for a representative flight-like module. This module is constructed with readouts from the low-noise Lot 3 run of CRC-696 readouts. Other developmental modules have significantly higher noise since they are made with alternate, higher noise lots. This read noise is attained with a total input node capacitance of nearly 3 pF.

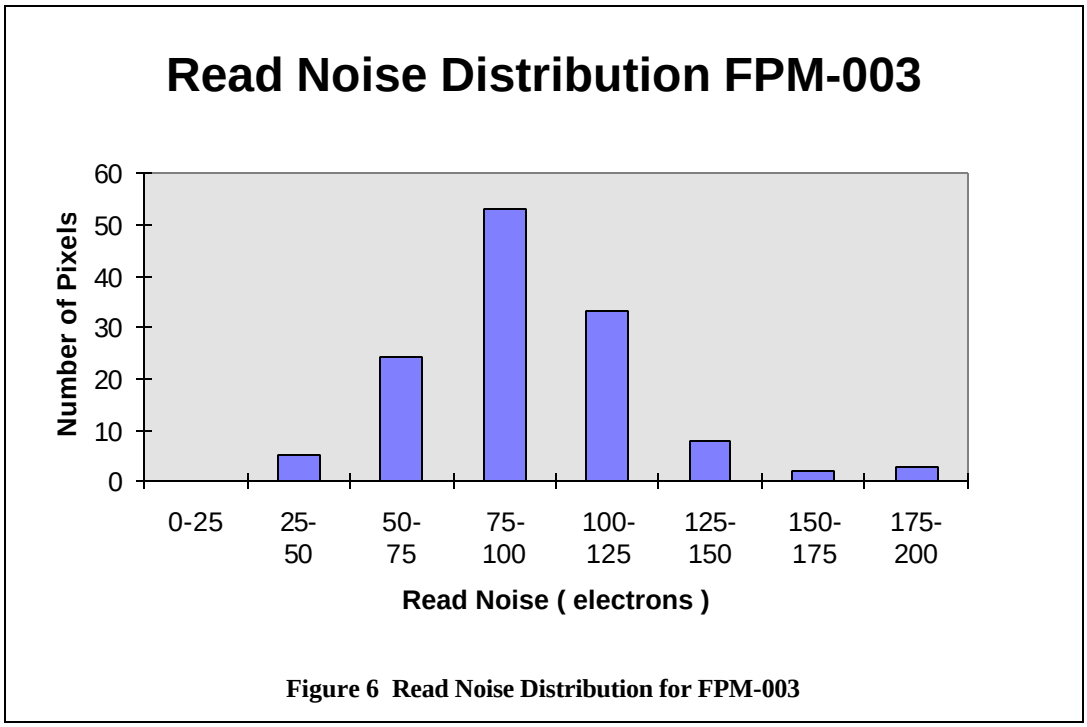

Figure 6 Read Noise Distribution for FPM-003

4.2 Dark Current

The dark current distribution for four modules is shown in Figure 7. The dark current is well below the expected natural background photocurrent of ~800 e/s.

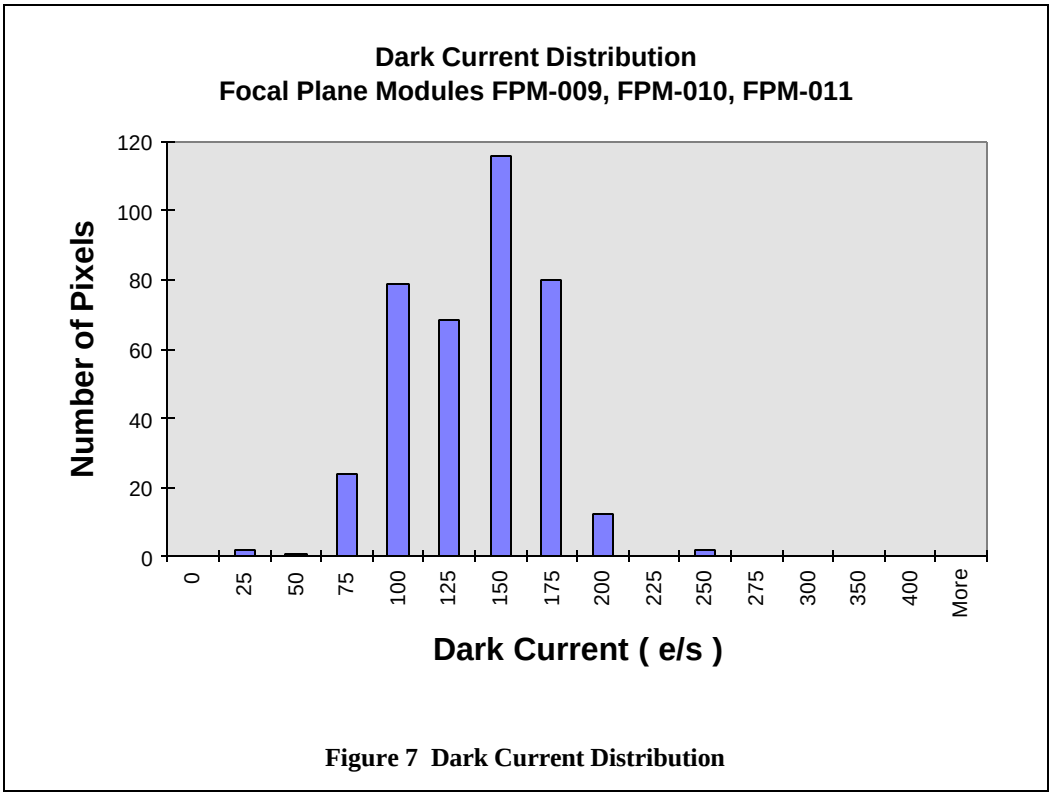

Figure 7 Dark Current Distribution

4.3 Power Dissipation

The standard operating current for the CRC-696 is 0.5 μA per input unit cell. Unlike a typical switched SFD circuit, it is necessary for the CTIA input stages to be on continuously. Hence, all 1024 input stages of the 32x32 array are dissipating power into the bath. Additionally, there is dissipation due to the digital circuitry and the output drivers for each readout. Table 2 summarizes the power dissipation in the array. In addition, the array requires power to perform the thermal anneal to restore responsivity after ionizing radiation exposure. Although the peak power for the anneal is 300 mW, the duty cycle is low enough (10 s every hour) to yield a time averaged anneal power dissipation of less than 1 mW.

Table 2 Array Power Dissipation (mW)

Unit Cell	Current Mirror	Digital Circuits	Output Driver	Total per Readout	Total per Array
26.4	1.6	< 1	12.5	40.5	1300

4.4 Full Well Capacity

The full well capacity is evaluated by observing the departure from linearity during an integration of a bright source. For the CTIA, saturation occurs abruptly at 2.8 x 10^5 electrons. Prior to that point, the ramp is linear to better than 1% since the bias on the detector is maintained constant by the negative feedback.

4.6 Electrical Crosstalk

An important consideration in operating in an ionizing radiation environment is the amount of electrical crosstalk in the array. Since the array is continuously being hit by energetic protons, the number of pixels "taken out" by a hit will have an impact on the true duty cycle (and hence integration efficiency) of the array. The SFD readout suffers from significant electrical crosstalk in our array geometry since the parallel lines at the input have parasitic cross capacitances of several tenths of pF. The CTIA is much better suited to this situation since the input potential held constant by the negative feedback. Hence, as

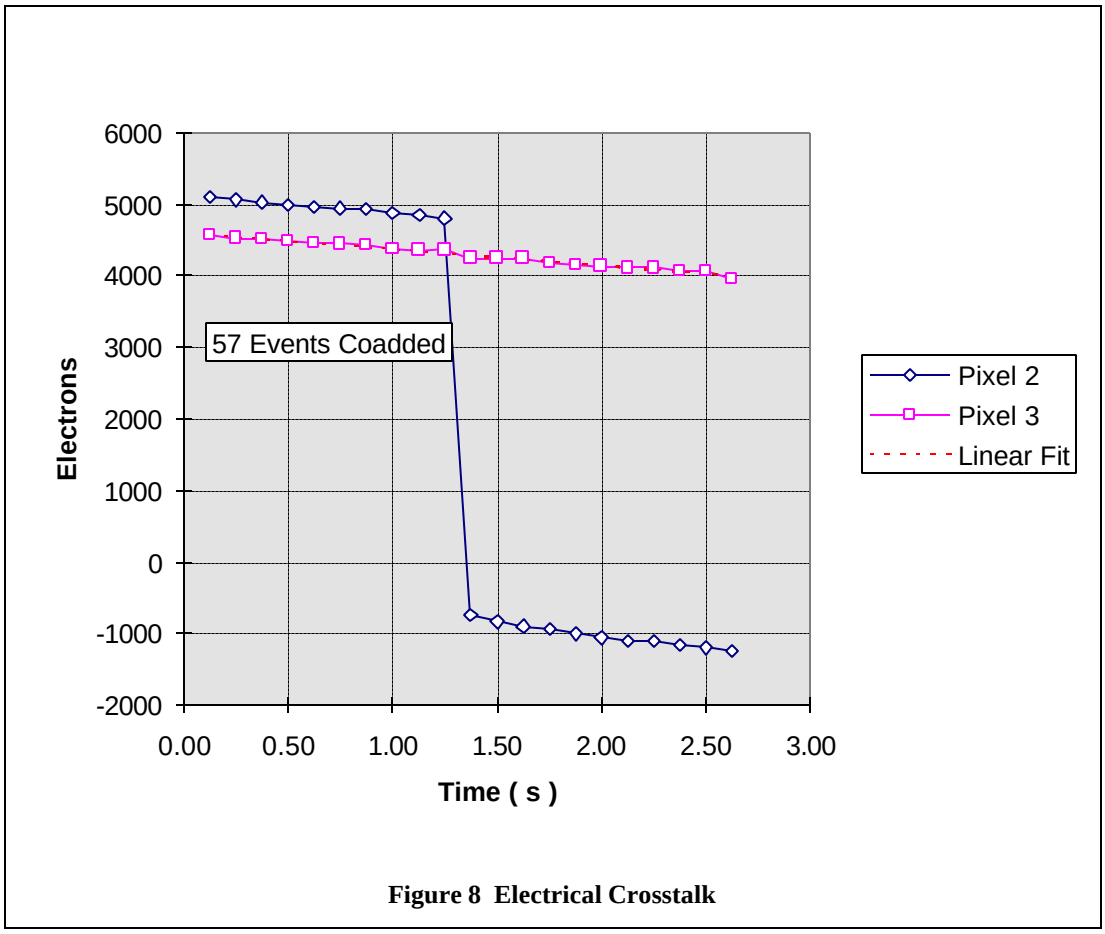

Figure 8 Electrical Crosstalk

long as the circuit is not saturated, there is virtually no electrical crosstalk. This performance is demonstrated in Figure 8. The figure shows the response to 60 MeV proton irradiation at the Crocker Nuclear Laboratory, University of California, Davis. The plot shows the discontinuity in the ramp due to a proton hit and the lack of crosstalk in the adjacent channel.

5. CURRENT STATUS

The 32x32 Ge:Ga array passed its critical design review for flight construction in December 1997. An important aspect of the readiness for flight construction is the installation of the required quality assurance methodology in our laboratory. The flight construction follows accepted aerospace practice of production travelers, detailed test procedures, release drawings, and quality monitoring. Preparations are being made to produce 24 flight quality focal plane modules as well as two backplane assemblies. Out of this set, the best eight units will be selected for the prime flight unit. The flight construction will begin in April 1998, leading to delivery of the flight and flight spare units in 1999. Subsequently, the focal plane array will be installed into the MIPS instrument at Ball Aerospace, leading to a launch of SIRTF in 2001.

ACKNOWLEDGEMENTS

The MIPS project is supported by the National Aeronautics and Space Administration under a contract from the Jet Propulsion Laboratory. We also acknowledge support from NASA under grant NAGW-1285.

REFERENCES

[1]R. Schnurr, C. L. Thompson, J. T. Davis, G. H. Rieke, E. T. Young, "Design of the stressed Ge:Ga far-infrared array for SIRTF", in Infrared Astronomical Instrumentation, A. M. Fowler, ed, ***Proc. SPIE, 3354***, ,1998.

[2] E.T. Young, M. Scutero, G.H. Rieke, and J. Davis, "Construction of the large-format far-infrared array for SIRTF" in ***Infrared Detectors and Instrumentation for Astronomy***, ed. A.M. Fowler, ***Proc. SPIE, 2475***, 441, 1995.

[3] E.T. Young, G.H. Rieke, and H.Dang, I. Barg, and C.L. Thompson, "Test Results for the SIRTF Far-Infrared Array Module", in ***Infrared Detectors and Instrumentation for Astronomy***, ed. A.M. Fowler, ***Proc. SPIE, 2475***, 435, 1995.

[4] M.G. Hauser, "The COBE DIRBE search for the cosmic infrared background", in International Astronomical Union Symposium no.168, p99-108,1996.